doi:10.1006/jmbi.2001.5057 available online at http://www.idealibrary.com on IDEAL® J. Mol. Biol. (2001) 313, 511–524

JMB

Dimerization of the 3′UTR of *bicoid* mRNA Involves a Two-step Mechanism

Céline Wagner[1], Isabel Palacios[2], Luc Jaeger[1], Daniel St Johnston[2] Bernard Ehresmann[1], Chantal Ehresmann[1]* and Christine Brunel[1]

[1]*UPR 9002 du CNRS, Institut de Biologie Moléculaire et Cellulaire, 15 rue Descartes 67084, Strasbourg Cedex France*

[2]*Wellcome/CRC Institute Tennis Court Road, Cambridge CB2 1 QR, UK*

**Corresponding author*

The proper localization of *bicoid (bcd)* mRNA requires *cis*-acting signals within its 3′ untranslated region (UTR) and *trans*-acting factors such as Staufen. Dimerization of *bcd* mRNA through intermolecular base-pairing between two complementary loops of domain III of the 3′UTR was proposed to be important for particle formation in the embryo. The participation in the dimerization process of each domain building the 3′UTR was evaluated by thermodynamic and kinetic analysis of various mutated and truncated RNAs. Although sequence complementarity between the two loops of domain III is required for initiating mRNA dimerization, the initial reversible loop-loop complex is converted rapidly into an almost irreversible complex. This conversion involves parts of RNA outside of domain III that promote initial recognition, and dimerization can be inhibited by sense or antisense oligonucleotides only before conversion has proceeded. Injection of the different *bcd* RNA variants into living *Drosophila* embryos shows that all elements that inhibit RNA dimerization *in vitro* prevent formation of localized particles containing Staufen. Particle formation appeared to be dependent on both mRNA dimerization and other element(s) in domains IV and V. Domain III of *bcd* mRNA could be substituted by heterologous dimerization motifs of different geometry. The resulting dimers were converted into stable forms, independently of the dimerization module used. Moreover, these chimeric RNAs were competent in forming localized particles and recruiting Staufen. The finding that the dimerization domain of *bcd* mRNA is interchangeable suggests that dimerization by itself, and not the precise geometry of the intermolecular interactions, is essential for the localization process. This suggests that the stabilizing interactions that are formed during the second step of the dimerization process might represent crucial elements for Staufen recognition and localization.

Keywords: RNA dimerization; RNA localization; RNA-protein interactions; *bcd* mRNA; Staufen

Introduction

Intermolecular RNA recognition through loop-loop interactions (kissing) plays important biological roles in various systems. In naturally occurring antisense RNAs, rapid kissing is used to initiate conversion to stable antisense-target RNA complexes. This is well documented in cases of the copy number regulation of procaryotic plasmids ColE1,[1] R1,[2] pMU720,[3] and ColIb-P9.[4,5] A loop-loop interaction between $tRNA_3^{Lys}$ and HIV-1 genomic RNA is essential for initiation of reverse transcription (see Isel *et al*.[6] and references therein). Loop-loop interactions between autocomplementary sequences occur between identical RNA molecules. This is the case for genomic RNA dimerization in HIV-1 and MoMuLV, which plays an important role in retroviral replication.[7–10] A cyclic hexamer of the 120 base prohead (pRNA) was shown recently to be needed for efficient *in vitro* packaging of the *Bacillus subtilis* bacteriophage phi29 genome.[11–13] Interestingly, intermolecular RNA loop-loop interactions have been proposed to be involved in the formation of ribonucleoprotein particles for transport and localization of the *bicoid* (*bcd*) mRNA.[14]

E-mail address of the corresponding author: Chantal.Ehresmann@ibmc.u-strasbg.fr

0022-2836/01/030511–14 $35.00/0

The establishment of the Bicoid morphogen gradient in early *Drosophila* embryos requires the prelocalization of *bcd* mRNA to the anterior pole of the egg. The program of *bcd* mRNA localization involves multiple steps during oogenesis and early embryogenesis. This multi-step process requires three known genes. Mutations in *exuperantia* and *swallow* disrupt *bcd* mRNA localization to the anterior cortex of the oocyte during oogenesis. Staufen is required from late oogenesis (stage 12) until early embryogenesis to anchor *bcd* mRNA,[15] as well as for its translational regulation.[16] Ferrandon and collaborators[17] proposed that endogenous Staufen associates specifically with *bcd* mRNA 3′ untranslated region (UTR) when injected into the early embryo, resulting in the formation of characteristic RNA-protein particles. These particles associated with astral microtubules during mitosis and formed bipolar patterns at metaphase that were visualized with a Staufen antibody.[17] Sequences both necessary and sufficient for the full localization program have been located within the *bcd* mRNA 3′UTR.[17,18] Regions within the *bcd* mRNA 3′UTR recognized by Staufen were mapped using a linker scanning strategy.[17] They were predicted to form three stem-loop structures involving long, double-stranded helices.[14,19,20] Moreover, intermolecular base-pairing involving two single-stranded loops has been proposed to play a major role in particle formation.[14] In parallel, it was shown that the *bcd* 3′UTR RNA is able to oligomerize *in vitro* at a high salt concentration.[14] The RNA elements responsible for promoting dimerization were suggested to lie between positions 211 and 353 (domain III) of the *bcd* mRNA 3′UTR. These observations led to the proposal of a simple model (Figure 1), in which base-pairing between conserved complementary sequences in the apical and side loops of domain III of two different molecules are required for Staufen binding.[14]

The present work represents the first attempt to gain insight into the mechanism of *bcd* 3′UTR dimerization. This includes the determination of the apparent dimerization dissociation (K_d) and dynamic parameters of mutated and truncated RNAs, as well as competition assays with antisense and sense oligonucleotides. Finally, the wild-type dimerization domain of *bcd* 3′UTR mRNA was substituted by heterologous dimerization motifs. All RNA mutants were tested for their ability to promote formation and transport of *bcd* mRNA-containing particles in living embryos. This was achieved by following fluorescently labeled RNAs in two transgenic *Drosophila* strains, expressing either a microtubule-associated protein or Staufen fused with the green fluorescent protein (GFP). This study provides new clues about the dimerization process and its functional implications.

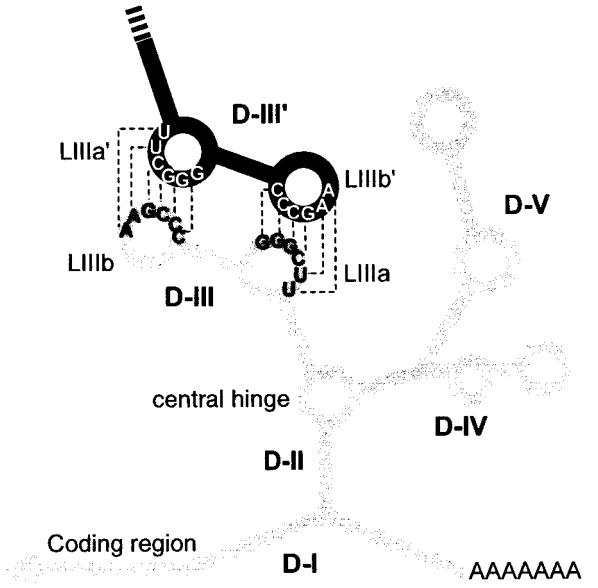

Figure 1. A representation of the 3′UTR secondary structure. The secondary structure is derived from computer prediction and sequence comparison,[19,20] and chemical probing (our unpublished results). The five domains (I to V) are indicated as well as the coding region and the poly(A) tail. Domain III of a second RNA molecule (D-III′) is shown with the proposed double loop-loop interactions.[14]

Results

Loops IIIa and IIIb play a pivotal role in promoting dimerization

A secondary structure model of the *bcd* mRNA 3′UTR has been derived from computer prediction and sequence comparison.[19,20] The organization into five independent domains (Figure 1) was mostly confirmed by enzymatic and chemical probing (our unpublished results). Briefly, domains II to V form a highly structured core, flanked by mostly single-stranded regions (domain I). In order to characterize the dimerization site and the contribution of the different domains of 3′UTR mRNA to the dimerization process, we measured the apparent dimerization dissociation constant (K_d) of different RNA variants (Figure 2 and Table 1). Both RNA fragments containing the complete 3′UTR RNA, with or without the 5′ extension arising from the polylinker plasmid (RNA 875′ or 875, respectively; Table 1), were found to dimerize with a similar K_d value (42 and 65 nM, respectively). The structured core RNA (RNA ΔI), was found to dimerize with an almost tenfold decreased K_d (Table 1, Figure 3(a)). Deletion of both domains IV and V (RNA Δ(IV + V)) had no significant effect on dimerization (Table 1), suggesting that neither domain IV nor V contains elements involved in the intermolecular interaction. As expected, deletion of domain III containing the putative dimerization

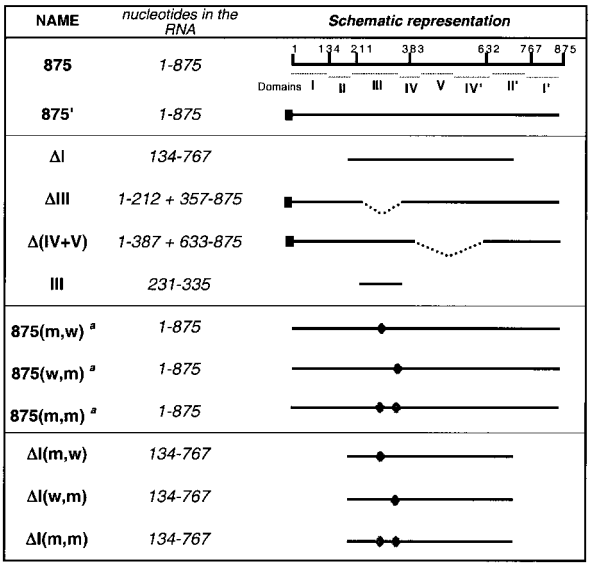

Figure 2. A representation of 3′UTR-derived RNAs. Number 1 refers to the first nucleotide right after the stop codon. The black squares indicate the presence of 72 additional nucleotides coming from the cloning vector. The gray diamonds indicate the location of mutations in domain III loops. Both versions of mutated RNA, with and without the 5′-terminal 72 additional nucleotides, were tested.

elements (RNA ΔIII) impaired dimerization. The isolated domain III (RNA III) was able to dimerize very efficiently. The K_d, which could not be determined precisely due to the formation of multimers, was estimated to be < 10 nM (Figure 3(b)).

The direct role of the two complementary sequences in loops IIIb and IIIa in the *in vitro* dimerization process was investigated by introducing mutations into loops IIIa and IIIb of domain III in RNA 875. AAGCCC282 and GGGCUU322 were substituted by AGUGAC (RNA 875(m,w)) and GUCACU (RNA 875(w,m)), respectively. These mutations, identical with those used by Ferrandon *et al.*,[14] were intended to disrupt base-pairing when introduced into one of the two loops, and to restore complementarity when introduced simultaneously into both loops (RNA 875(m,m)). As expected, mutations in one of the two loops impaired dimerization strongly (Table 1). Introduction of the two compensatory mutations (RNA 875(m,m)) was able to restore dimerization properties (Table 1).

Because dimerization was estimated by retardation on agarose gel electrophoresis, it was necessary to ascertain that the retarded band did correspond to an RNA dimer and not to a different conformer induced by the high salt concentration. We used RNA 875′ and RNA Δ(IV + V), one of which being alternatively labeled, and followed the formation of a labeled heterodimer, in addition to the expected homodimers. Indeed, co-incubation of the two RNAs leads to the formation of a new labeled band that migrates between the two homodimers (not shown), and this corresponds to a heterodimer between RNAs 875′ and Δ(IV + V). Intermolecular interactions were further supported by rescue experiments *in trans*. In these experiments, a low concentration of labeled RNA 875(m,w) or (w,m) was incubated with increasing concentrations of the unlabeled ''*trans*-compensatory'' RNA (RNA 875(w,m) or (m,w)). The formation of the heterodimer was followed by quantifying the retarded labeled band, and the K_d deduced for heterodimerization was similar to that measured for wild-type dimerization (Table 1). A similar behaviour was observed in both RNA 875′ and RNA ΔI contexts (Table 1).

Table 1. Dimerization parameters of the RNAs

RNA	K_d (nM)	$t_{ass}1/2$ (min)	$t_{diss}1/2$ (min)	Particle formation
875	65			+++
875′	42	12	>60	+++
ΔI	5	2.5	>60	+++
ΔIII	≫300			−
Δ(IV + V)	38		>60	−
III	<10[b]		0.8	
875′(m,w)[a]	≫300			−
875′(w,m)[a]	≫300			−
875′(m,m)[a]	78			+++
875′(m,w) + 875′(w,m)*	57			
875′(m,w)* + 875′(w,m)	55			+++
ΔI(m,w)	64			
ΔI(w,m)	≫300			
ΔI(m,m)	14			

The apparent K_d values are indicated (with ±50% as a standard error). Kinetic parameters are defined as follows: $t_{ass}1/2$ is the time-lapse for the formation of 50% of dimer, $t_{diss}1/2$ is the time-lapse for the dissociation of 50% of dimer. The capability of the injected RNAs to form localized particle containing Staufen *in vivo* is indicated by +++ for a pattern identical with wild-type, and by − when no particle is formed. The RNA species denoted by an asterisk (*) was ^{32}P-labeled.

[a] RNAs lacking the 5′-terminal 72 additional nucleotides from the vector led to similar results.

[b] The K_d value was estimated from dimer + multimer formation.

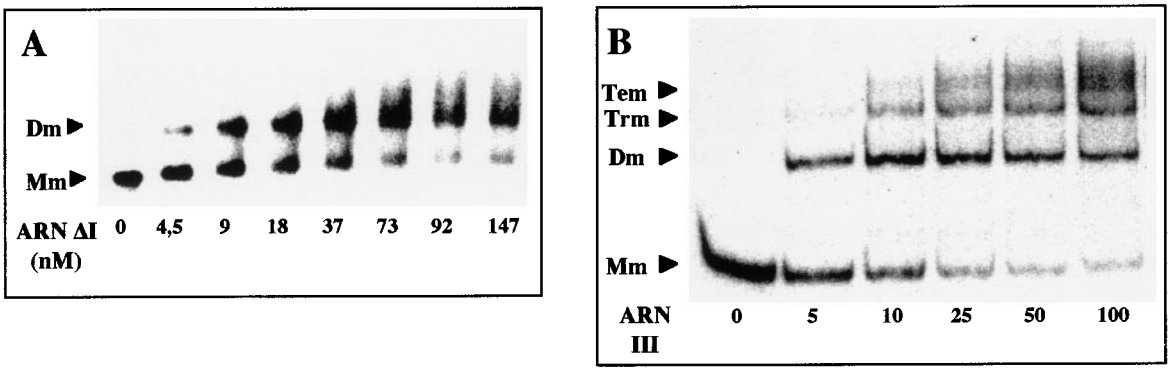

Figure 3. Effect of various deletions on RNA dimerization. (a) Dimerization as a function of RNA ΔI concentration; (b) multimerization as a function of RNA III concentration. The monomeric (Mm), dimeric (Dm), trimeric (Trm) and tetrameric (Tem) forms were fractionated by agarose gel electrophoresis and treated as described in Materials and Methods. O indicates that no unlabeled RNA was added.

Dissociation and association kinetics suggest a two-step mechanism

To get more information about the observed differences in K_d, we compared the kinetic parameters of dimerization. RNAs were uniformly labeled with ^{32}P and dimer formation was allowed under standard conditions. For association experiments, RNA 875 and RNA ΔI were incubated at 125 nM and aliquots were removed at various times and analyzed by agarose gel electrophoresis (Figure 4(a) and (b)). Dimerization of the full-length RNA 875 appeared to be a rather slow process, as 50 % of dimerization was attained after 12 minutes of incubation. The dimerization of RNA ΔI was markedly faster, since 50 % of dimerization was attained after two to three minutes of incubation. The association kinetic of RNA III was more difficult to evaluate because of multimer formation. However, RNA III (incubated at 50 nM) was found to dimerize much faster than RNAs 875 or ΔI, since a maximum level of dimer was reached after only one minute (results not shown).

For dissociation experiments, RNAs were first allowed to dimerize for 30 minutes. RNA III was incubated at 5 nM, a concentration yielding only dimers (Figure 4(b)). Dissociation was then achieved by 50-fold dilution in dimerization buffer. The final concentration was below the measured K_d values (at least tenfold). It was further verified that no detectable dimer was formed under these conditions (Figure 4(c) and (d), lane CT). Aliquots were removed at various times and analyzed by gel agarose electrophoresis (Figure 4(c) and (d)). It appeared that dimers formed either with RNAs 875, ΔI or Δ(IV + V) did not dissociate within the incubation time (60 minutes) (Table 1). These experiments revealed an unexpected stability of the dimer once formed, which is independent of the presence of domain I, V and part of domain IV. In contrast, RNA III dimer dissociated rapidly (Table 1), indicating that dimerization of this short RNA is a reversible process, as expected from a simple loop-loop recognition process.[21,22] These results suggest that dimerization is most likely initiated by reversible loop-loop interactions involving domain III. This dynamic complex is subsequently converted into an almost irreversible dimer.

Antisense and sense oligonucleotides are unable to inhibit dimerization once conversion has proceeded

Since the dimer obtained after the conversion step is very stable, we expected that molecules designed to interfere with dimerization would not be able to inhibit dimerization once stabilization has proceeded. Thus, we tested the ability of antisense or sense oligonucleotides to inhibit dimerization of RNA875′, when added before or after formation of the dimer. We first used an antisense DNA oligonucleotide complementary to nucleotides 270 to 283 (AS-LIIIb). This oligonucleotide exerted a strong inhibitory effect (76 % inhibition at a 1:1 molar ratio, not shown), provided that it was added before the dimerization step (before or after the denaturation/renaturation step). However, when the antisense oligonucleotide was added (up to a 70-fold molar excess) to the preformed dimer, no inhibition was observed, even after 30 minutes of incubation. Then, we tested the ability of short sense competitor RNAs (S-LIIIb and S-LIIIa) to interfere with dimerization of RNA 875′. When added before the dimerization step, both sense RNAs were able to inhibit dimerization, although with a reduced efficiency as compared to AS-LIIIb (half inhibition attained at a 10:1 molar ratio, not shown). However, both sense RNAs failed to interfere with dimerization when added after dimerization was completed. Thus, both types of competitor oligonucleotides can interfere only with the initial loop-loop interaction, but not after conversion has proceeded.

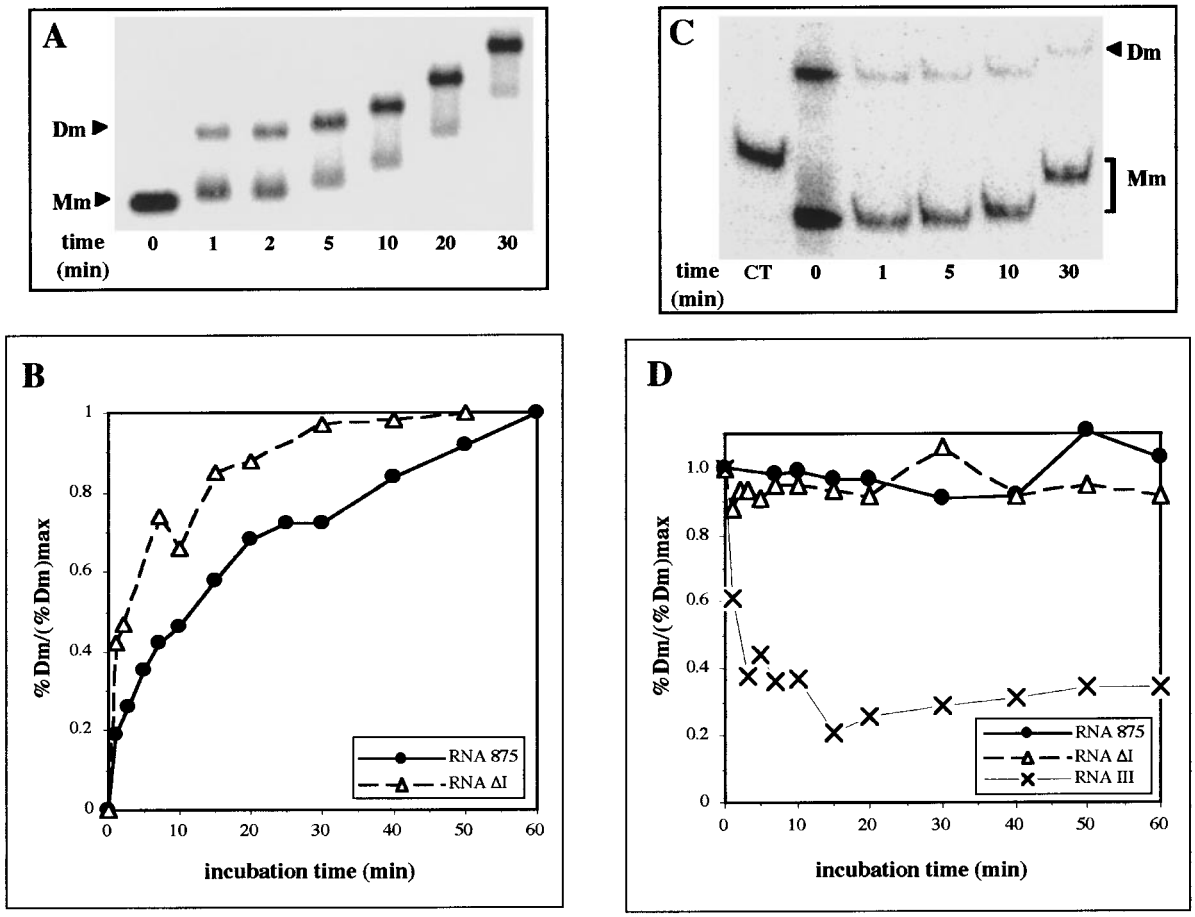

Figure 4. Kinetics of association and dissociation of RNA variants. (a) and (b) Kinetics of dimer formation. (a) Autoradiograph of the fractionation gel showing monomer (Mm) and dimer (Dm) species of RNA ΔI as a function of time (aliquots are loaded onto the gel at different times). Time 0 is obtained by taking an aliquot immediately after addition of the dimer buffer. (b) Kinetics of dimer formation of RNA 875 and RNA ΔI. Results are expressed as the weight-to-weight ratio of the dimers formed at a given time to the level of dimers formed at the plateau. (c) and (d) Kinetics of dimer dissociation. (c) Autoradiograph of the fractionation gel showing dimeric (Dm) and monomeric (Mm) forms of RNA III as a function of time after dilution. CT is an incubation control showing that no dimer was formed when the RNA was incubated for 30 minutes at the final concentration obtained after dilution. Time 0 was obtained by running an aliquot of the dimerization mixture immediately before dilution. (d) Results are expressed as the weight-to-weight ratio of the remaining dimer to dimer formed at time 0. Symbols are indicated in the insets.

Correlation between *in vitro* dimerization and the formation of localized particles containing Staufen

Ferrandon and co-workers previously showed that injection of *bcd* 3′UTR mRNA resulted in the formation of characteristic particles containing endogenous Staufen.[14,17] The particles, observed in fixed embryos with a Staufen antibody, formed bipolar patterns at the site of injection.[17] Here, we set up an improved injection assay that allowed us to follow the fate of the injected RNA directly in real time in living embryos. In this assay, *in vitro* transcribed RNAs labeled with rhodamine were injected into a small region of the cytoplasm of a less than one hour-old embryo. The formation and transport of the labeled RNA containing particles was monitored for several consecutive mitotic divisions under a confocal microscope. All experiments were performed in parallel in two *Drosophila* transgenic strains. The first expressed a fusion protein between GFP and MAP-Tau.[23] This strain allowed us to observe the transport of RNA-containing particles along the mitotic spindles, and the formation of bipolar patterns at metaphase. This is illustrated in Figure 5(a), in which RNA 875 formed localized particles (in red) concentrated around both poles of the mitotic spindles at metaphase, in close proximity to the astral microtubules that emanate from each spindle pole (in green). This localization was specific, since injection of either *bcd* antisense RNA or snRNA U1, a highly structured RNA, did not promote particle formation. The second strain, which expressed a GFP-Staufen fusion protein,[24] allowed us to visualize the recruitment of Staufen to the localized particles and its co-localization with the injected labeled

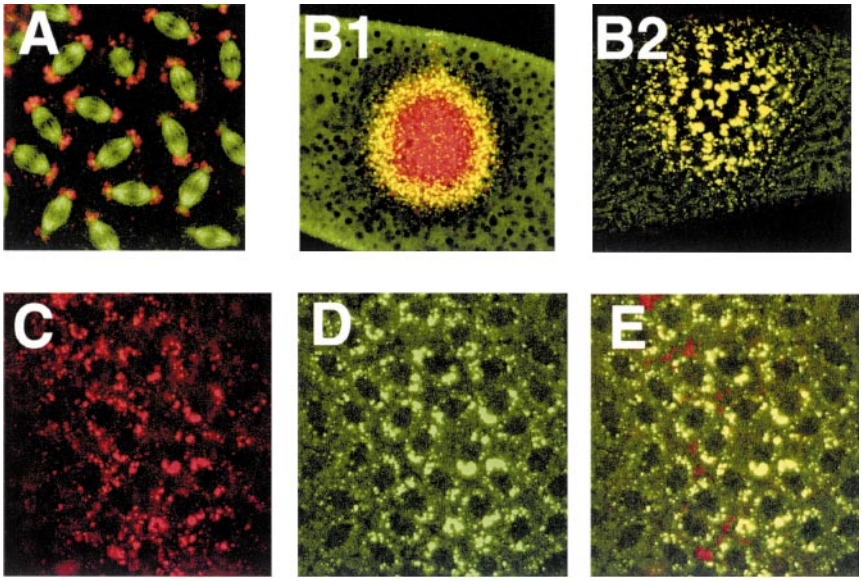

Figure 5. Formation of localized ribonucleoparticles to astral microtubules of mitotic spindles. RNA 875 labeled with rhodamine was injected in all cases. (a) Injection of RNA in young tau-GFP embryos: localization of the tau-GFP protein is observed as the green signal, and the injected RNA as the red signal. (b1-2) Recruitment of Staufen in localized particles upon injection of RNA in young Stau-GFP embryos as mitosis proceeds. The Staufen-GFP protein is observed as the green signal, the injected RNA as the red signal, and ribonucleoproteins containing both RNA and Staufen-GFP as the yellow signal: within a few minutes (b1) or 30 minutes (b2) after RNA injection. (c)-(e) Co-localization of RNA and Staufen in young Stau-GFP embryos: (c) specific signal of RNA (in red); (d) specific signal for Staufen protein (in green); (e) merging of both signals (in yellow).

RNA. Indeed, direct evidence for co-localization was provided by the simultaneous occurrence of both RNA and GFP-Staufen fluorescences, resulting in the formation of yellow particles. The time-dependent formation of these doubly labeled particles is illustrated in Figure 5(b). Particles containing labeled RNA 875 and GFP-Staufen were visible around the site of injection after a few minutes (Figure 5(b1)) and localize to the poles of the mitotic spindles when they form (Figure 5(b2)). Co-localization of RNA and GFP-Staufen is further illustrated in Figure 5(c)-(e). It is noteworthy that labeling of the RNA did not interfere with the formation of Staufen-containing particles.

The possible functional link between RNA dimerization, formation of localized particles and recruitment of Staufen was tested by analyzing all the RNA variants tested *in vitro* for their dimerization properties, using the injection assay described above. The results are summarized in Table 1. Injection of RNA ΔI gave a bipolar pattern of Staufen-containing particles indistinguishable from RNA 875. In contrast, deletions of domain III (RNA ΔIII) or of domains IV and V (RNA Δ(IV + V)) abolished particle formation and recruitment of Staufen. Injection of either 875(m,w) or (w,m) RNA alone did not lead to particle formation, whereas particle formation was restored when the *cis*-complementary double mutant RNA (RNA 875(m,m)) was used. Furthermore, *trans*-complementation was observed by co-injecting RNAs 875 (m,w) and (w,m), one of which was labeled with rhodamine while the other one was unlabeled. These results are in complete agreement with those obtained by Ferrandon *et al.*[14,17] Finally, a mixture of RNA 875 and antisense oligonucleotide AS-LIIIb was injected into embryos. The oligonucleotide exhibited a concentration-dependent inhibitory effect on particle formation, and a complete inhibition was observed upon injection of an [RNA]/[oligonucleotide] ratio of 1:100 (Figure 6), indicating that elements that are required for *in vitro* dimerization are essential also for *in vivo* particle localization.

Heterologous dimerization motifs can substitute for the homologous one

To test the specific contribution of *bcd* RNA dimerization on particle formation and transport, we constructed chimeric RNAs in which the homologous dimerization domain was substituted with heterologous dimerization motifs (Figure 7(a)). The first one, encompassing the tetraloop GAAA and its helicoidal receptor, was identified in group I introns.[25,26] As in the case of *bcd* mRNA, dimerization proceeds througth a bipartite site separated by an irregular helical region of similar length. Thus, this module was expected to generate a geometry close to that proposed for the *bcd* RNA-RNA interaction, as suggested by three-dimensional modeling of the *bcd* dimerization[14] and the loop/receptor[26] motifs (Figure 7(b)). The loop/receptor module was substituted for nucleotides 241 to 33 of domain III (RNA 875-L/R).

The second heterologous sequence corresponds to the dimerization initiation site (DIS) of the HIV-1Lai genomic RNA, which dimerizes through a single loop-loop interaction. The topology of such a dimer should be totally different from the native one or from that formed by the tetraloop receptor (Figure 7(b)). Indeed, it was expected to yield an almost co-axial stacking of the resulting helices, as suggested by RNA probing and modeling,[27] NMR

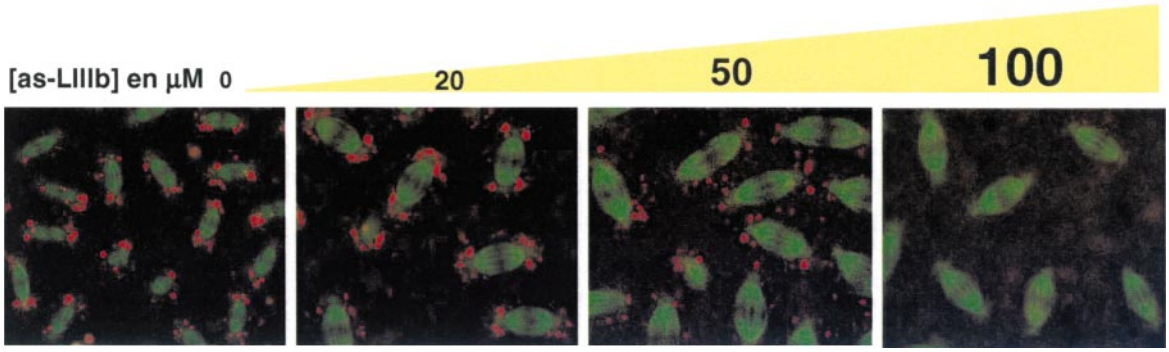

Figure 6. Inhibition of the formation of localized particles by antisense oligonucleotide AS-LIIIb. An increasing amount of the AS-LIIIb oligonucleotide was injected with rhodamine-labeled RNA 875 in tau-GFP embryos. Same signals as in Figure 5(a).

studies[28,29] and recent X-ray crystallography data (E. Ennifar, P. Walter, B.E., C.E. & P. Dumas, P., unpublished results) on the HIV-1 DIS. The HIV-1 DIS was substituted for nucleotides 251 to 304 (RNA 875-HIV) or 256 to 298 (RNA 875-HIV′), differing by half a helix turn. In each case, the substitution site of the heterologous domain was chosen to maintain a length similar to that of the wild-type domain III. Incidentally, a variant of RNA 875-HIV was obtained after the PCR reaction, that displayed a point mutation in the autocomplementary sequence of the apical loop and a four nucleotide deletion in the stem (RNA 875-HIVmut, Figure 7(a)). This mutant was predicted to have altered dimerization properties. According to enzymatic probing, the inserted heterologous motifs folded as the expected stem-loop structure (data not shown).

Interestingly, RNA 875-L/R dimerizes with an apparent K_d value (Figure 7(a)) much lower than that of the isolated GAAA-receptor module.[26] This observation suggests that additional interactions occur to stabilize the dimer formed, as in the wild-type *bcd* RNA (see above). In agreement with this idea, this chimeric dimer did not dissociate within 60 minutes of incubation (data not shown). On the other hand, chimeric RNA 875-HIV and 875-HIV′ were able to dimerize with an apparent K_d close to that measured for a HIV-1 RNA fragment containing the DIS[30] (Figure 7(a)). As expected, dimerization of RNA 875-HIVmut was reduced as compared to RNA 875-HIV (Figure 7(a)). The dimers formed with RNA 875-HIV or 875-HIV′ did not dissociate during 60 minutes of incubation (data not shown). Since the initial DIS interaction is known to be reversible [30,31], this indicates that the conversion into a stable form also proceeds, although the initial kissing interaction was designed to yield a geometry different from that of the wild-type *bcd* RNA.

When injected, chimeric RNAs 875-L/R, 875-HIV and 875-HIV′ were able to induce the formation of localized particles (Figure 7(c)). Moreover, double labeling of Staufen (*via* the GFP) and the injected RNAs (*via* the rhodamine) demonstrated the perfect co-localization of both molecules (Figure 7(d)). In contrast, RNA 875-HIVmut displayed marked defects in the localization process (Figure 7(c) and (d)), demonstrating that the ability to form localized particles *in vivo* depends on the capacity of the RNA to dimerize.

Discussion

Dimerization of *bcd* mRNA involves at least two steps

Our results confirm data reported by Ferrandon *et al.*,[14] pointing to domain III as the element that triggers *bcd* mRNA 3′UTR dimerization through loop-loop interaction. The requirement for sequence complementarity between loops IIIa and IIIb in promoting RNA dimerization was confirmed by the use of *cis* and *trans*-complementary mutants. While domains IV and V are dispensable for RNA dimerization, domain I reduces the dimerization efficiency. This latter observation is in agreement with results obtained from HIV-1, where the K_d measured for a large RNA fragment containing the dimerization site was higher than that of the isolated dimerization element.[32] According to kinetic studies, the negative effect of domain I on K_d is attributed to a reduction of the association rate. This might correlate with the observed flexibility of domain I, which may impede productive collisions between the two RNA molecules simply by steric hindrance. This is not necessarily the case *in vivo*, because domain I is known to contain several regulatory *cis*-elements recognized by different proteins, and is therefore probably not free.

In addition, the present study provides new information about the mechanism of dimerization, which appears to be more complex than previously thought. The fact that domain III, the driving element of dimerization, forms reversible dimers (as expected for a loop-loop interaction) while larger fragments do not, suggests that the initial recognition is triggered by dynamic kissing and that the loop-loop dimer undergoes a maturation step

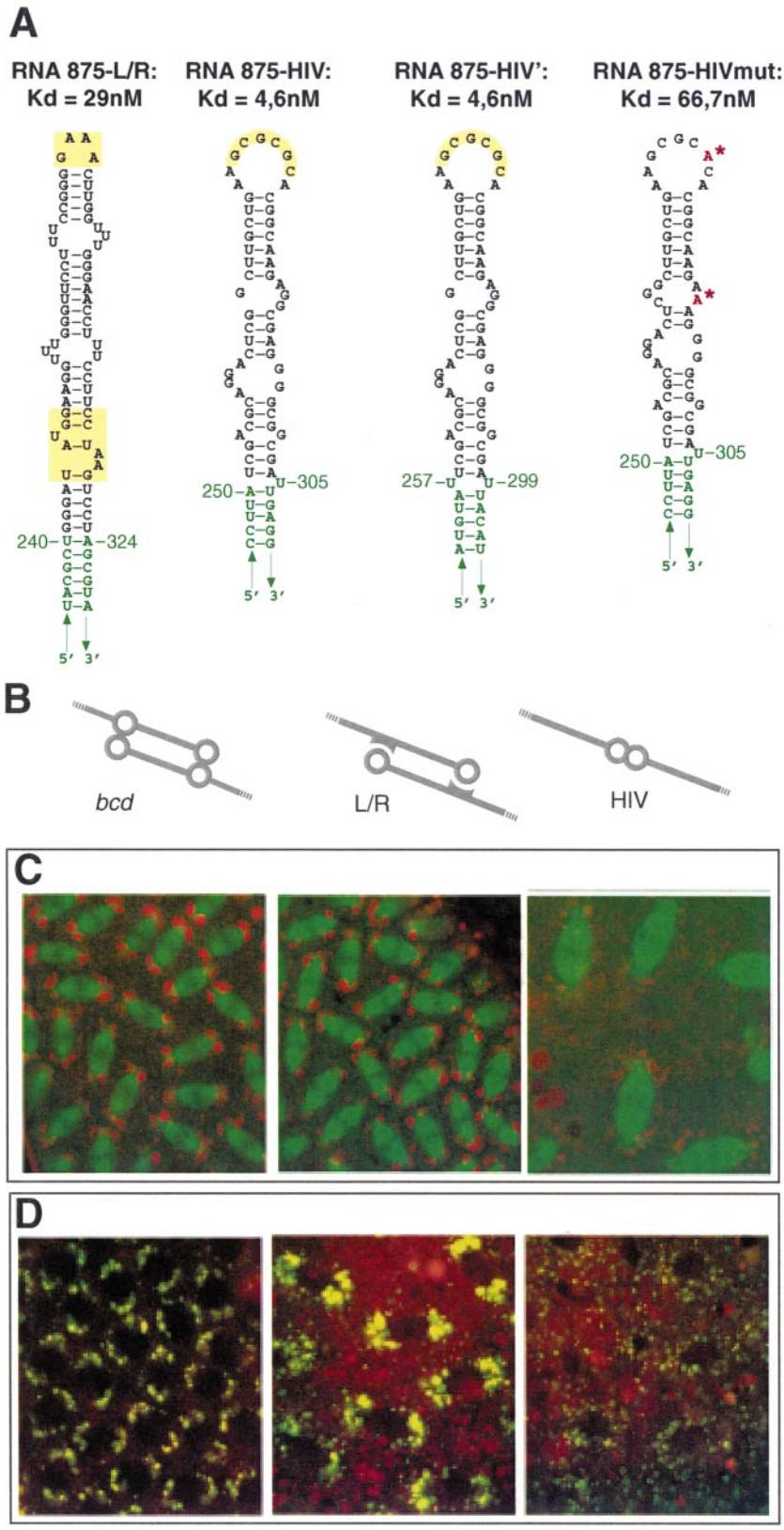

Figure 7. Chimeric RNAs promote dimerization *in vitro* and particle localization. (a) Sequence and secondary structure of the different dimerization modules substituted for *bcd* 3′UTR domain III. The site of insertion is shown, with *bcd* RNA nucleotides in green. The sequences responsible for intermolecular interactions are in yellow boxes. The nucleotides written in red and indicated by a star are the nucleotides mutated compared to the wild-type HIV-1 DIS sequence. The corresponding apparent K_d of chimeric RNAs. (b) A representation of the topology of the dimers expected to be provided by the different dimerization modules. (c) Injection of chimeric RNA 875-L/R (left panel), RNA 875-HIV RNA (central panel) and 875-HIVmut (rigth panel) labeled with rhodamine into a tau-GFP embryo (same signals as in Figure 5(a). (d) Injection of chimeric RNA 875-L/R (left panel), RNA 875-HIV (central panel) and RNA 875-HIVmut (rigth panel) labeled with rhodamine into a Staufen-GFP embryo (merging of RNA and Staufen-GFP signals as in Figure 5(e)).

leading to an almost irreversible complex. This is fully confirmed by competition experiments with sense and antisense oligonucleotides. First, sense and antisense oligonucleotides, targeted against loops IIIa and IIIb, inhibit dimerization with different efficiencies (antisense oligonucleotides being more efficient than sense RNAs), reflecting different competition mechanisms. Sense RNAs are

assumed to act as competitive inhibitors, interfering with dimerization through the loop-loop recognition step, while antisense oligonucleotides are assumed to inhibit dimerization through a mechanism that does not use loop-loop recognition.[33,34] Therefore, the inhibition observed with sense RNA provides an additional support for the involvement of the proposed kissing interactions in the early step of the dimerization mechanism. Second, both sense and antisense oligonucleotides are able to interfere with dimerization only during the initial reversible loop-loop recognition step, and become inefficient once the transition through the stable dimer has proceeded. Otherwise, it appeared from deletion experiments that domain I and the major parts of domains IV an V are dispensable for the transition to the stable complex. Therefore, the stem of domain II, the large hinge region, and part of helix IVa should be involved in the stabilization process. The nature of the stabilizing interactions is unknown, and the mechanism of conversion of the kissing complex to a highly stable complex raises a number of interesting questions about RNA folding and formation of intermolecular interactions.

The most unexpected finding was that substitution of the dimerization motif of domain III by heterologous dimerization motifs of different geometry (the loop/receptor motif and the HIV-1 DIS) also permits dimerization. Moreover, these motifs allow dimerization, and are able to trigger the stabilization process. Both *bcd* and loop/receptor motifs are expected to yield a side-by-side alignment of helices,[14,26] while the loop-loop HIV-1 motif generates coaxial alignment of helices[27–29] (E. Ennifar, P. Walter, B.E., C.E. & P. Dumas, unpublished results) (Figure 7(b). Although the local topology of the intermolecular interactions differ strongly, helix Illa of each molecule might be oriented in an overall similar orientation. Thus, we can assume that the local differences at the interacting sites can be compensated by the great flexibility of the hinge region, allowing additional contacts and/or rearrangements to occur.

A two-step (or multi-step) mechanism has been observed in several biological systems, such as genomic RNA dimerization of HIV-1 and binding of natural antisense RNAs. In the first case, it was shown that dimerization was initiated by a loop-loop interaction.[8,30,31,35,36] The kissing complex is then thought to be converted into an extended duplex by the nucleocapsid domain of the Gag protein.[37,38] Otherwise, downstream sequences increased the thermal stability of the dimer *in vitro*.[30] In the case of natural antisense RNAs, the binding pathway includes several steps, starting from a reversible loop-loop interaction, then leading to an irreversible and inhibitory complex.[1–5] In the case of the regulation of plasmid R1 replication, the initial kissing interaction is converted spontaneously into extended interactions, involving directional helix progression and disruption of the initial interaction, leading to the formation of a stable four-way junction.[39,40]

RNA dimerization, formation of localized particles and Staufen recruitment

Staufen is required late in oogenesis to anchor the *bcd* mRNA to the anterior pole of the fertilized egg[15] and to regulate its translation.[16] Staufen is known to contain five double-stranded RNA-binding domains (dsRBD). Binding of the third dsRBD to helical RNA was shown to require a minimum of eight continuous base-pairs.[41] The NMR structure of this binding domain bound to an RNA stem-loop revealed that RNA recognition is essentially driven by the shape of the A-form helix through interactions in the minor groove and phosphodiester backbone.[41] Recently, it was shown that the loop of dsRBD 2, in addition to dsRBD 3 and 5, is necessary for anchoring *bcd* mRNA to the anterior pole of the embryo.[16] Otherwise, *cis*-elements in *bcd* 3′UTR mRNA involved in Staufen recruitment were mapped by analyzing the effect of sets of disrupting and compensatory mutations on both strands of helices on the formation of localized Staufen-containing particles.[14] Mutation on one strand of helices IIIa, IIIb or IVb inhibited particle formation, while restoration of base complementarity was able to restore association with Staufen in localized particles, despite the substantial changes in the primary sequence of the RNA. However, the double mutation DF508 (UAAGA575/UCUUA587) in domain IV failed to restore the ability to form Staufen-containing particles.[14] These results suggest the presence of a sequence-specific element, required for particle formation. Inasmuch as this element is dispensable for dimerization, it might be involved in Staufen recruitment or some other step of the localization process.

Using an injection assay which allows us to simultaneously detect RNA and Staufen in living embryos, we could establish unambiguously a correlation between the ability of *bcd* mRNA to dimerize *in vitro* and to form localized particles containing Staufen *in vivo*. Indeed, all elements preventing dimerization *in vitro* (mutations, antisense oligonucleotides) impaired particle formation. Furthermore, both dimerization and particle formation were restored by the same elements (*cis* or *trans*-complementary mutations). Thus, the presence of RNA and Staufen in localized particles appeared to be intimately linked. However, if dimerization is necessary for particle formation, it is not sufficient, since domains IV and V are dispensable for dimerization, but required for particle formation, indicating that these domains contain one (or more) important signal for localization (see below).

Our findings that chimeric RNAs containing heterologous dimerization domains are competent in forming particles and in recruiting Staufen indicates that the ability of the RNA to dimerize *per se* is more important than the geometry of the intermolecular interaction at the dimerization site. In addition, they shed new insights on Staufen recognition. In particular, they suggest that the initial

dimerization site is probably not recognized specifically by Staufen. However, we cannot exclude the possibility that the substituted helical regions might be able to sustain binding. Taken together, these data favored the existence of multiple poorly specific interactions between helical regions of the RNA and the dsRBDs of Staufen, that would confer a good global affinity. The specificity of Staufen binding could be provided essentially by the three-dimensional arrangement of the RNA domains and the recognition of an array of weak interactions with the helical backbone. The stabilizing interactions that are formed during the second step of the dimerization process (which appear to occur in the chimeric RNAs) might represent crucial elements for Staufen recognition and localization.

What role for *bcd* mRNA 3′UTR quaternary structure?

Dimerization of *bcd* mRNA addresses numerous unanswered questions about its biological role in RNA localization. In the case of retroviral RNAs, the ubiquitous dimerization of genomic RNA is essential because it favors recombination between reverse transcription,[42] and it is involved in the selective packaging of the genomic RNA.[43,44] Mutation or deletion of the stem-loop involved in the initiation of dimerization induced severe defects in encapsidation and synthesis of proviral DNA.[7,10,45] It might be significant that genomic RNA has to escape translation and be selectively transported to the membrane of the infected cell for virion assembly. However, these steps are poorly understood. Recently, a small RNA called pRNA for ''packaging'' RNA, was identified to gear phage phi29 DNA translocation machinery across the capsid boundary.[46] Interestingly, pRNA contains two complementary loops that lead to the assembly of hexamers through ''hand-by-hand'' interactions.[12,13,47] The hexamer is built on the capsid from dimer units and the interacting loops play a key role in recruiting the incoming dimer.[13] The mechanism by which pRNA imparts rotational motion of the portal is still a matter for discussion.

Intermolecular interactions of *bcd* mRNA also involve two complementary loops that can potentially lead to the formation of multimers through hand-by-hand interactions. Consistent with this view, the isolated domain III was able to form multimers. However, only monomeric and dimeric species were observed as discrete bands with larger RNAs. Steric hindrance provided by the other structured domains or conversion of the initial loop-loop interaction into a stable dimer may impede multimerization. Furthermore, our finding that domain III can be substituted by heterologous domains that cannot form multimers but still promote dimerization *in vitro* and localized particles formation *in vivo*, indicates that the functional unit is a dimer.

As sequences involved in the intermolecular base-pairing are conserved within *Drosophila* species, this strongly suggests that dimerization is conserved throughout evolution. *bcd* mRNA dimerization would be an economic way for delivery and/or storage in the oocyte and the embryo, providing an architectural basis for the formation of the localized ribonucleoprotein particles, such as those we observe in *Drosophila* embryos. Nucleoprotein particles have been observed in many instances of mRNA transport, suggesting that particle formation may play an important role in packaging the RNA for efficient localization (for a review, see Bashirullah *et al*.[48]). However, the exact assembly pathway of the particles and its relation with the motor that transports the RNA complex is not understood. Another consequence of RNA dimerization is to generate an intrinsic duplication of *cis*-acting signals within the 3′UTR. A requirement for duplication of regulator binding sites has been observed experimentally with the BLE1 element. Indeed, two copies of this element are necessary to sustain early steps of localization of the *bcd* mRNA.[49] Thus, RNA quaternary structure might play a fundamental role in the binding of Staufen and other regulatory protein binding to *bcd* mRNA.

Materials and Methods

Plasmid construction and enzymatic digestion for *in vitro* transcription

Plasmid construction and restriction enzyme (Boehringer) digestions were conducted according to standard procedures.[50] RNAs used in this study (Figure 1) were transcribed from the following plasmids. The sequence of the different PCR primers used in this study is given in Table 2.

Plasmid 875 series

PCR was performed on pDF400, pDF495, pDF498 and pDF496 (kindly provided by D. Ferrandon[14]) using primers 1 and 2, and the generated *bcd* DNA fragments were cloned into the *Eco*RI-*Bam*HI sites of pUC18 to produce wild-type RNA 875, and mutants 875-(m,w), 875-(w,m), and 875-(m,m) respectively.

Plasmid 875′ series

The *Bst*NI fragment (positions 1 to 138 of the *bcd* 3′UTR) of pDF400 was subcloned into the *Stu*I site of the pUT8 vector, a pUC18 derivative containing a phage T7 RNA polymerase. The *Mlu*I-*Eco*RI fragment of pDF400 was cloned into the *Acc*I site of plasmid pUT8-bcd(1-138). The 875′-(m,w), 875′-(w,m), and 875′-(m,m) mutants were generated by exchanging the *Eco*RV-*Eco*RI fragment of the 875′ wild-type construct with the *Eco*RV-*Eco*RI fragment of the pDF498, pDF495, pDF496 plasmids.

Plasmid ΔIII

The *Eco*RV-*Eco*RI *bcd* fragment of the plasmid containing the RNA 875 was inserted into the pUC18 *Eco*RV-

Table 2. PCR primers used to constructs the different plasmids used in this study

Name	Sequence
1	5′CGAGATCGCGGATCCTCTAGAAAGGGACGGAAATATGG3′
2	5′CGAGATCCGGAATTCTAATACGACTCACTATAGGCCTGGACGAGAGGCGTG3′
3	5′GAATTCTAATACGACTCACTATAGGAATACGCTATTGCGCTT3′
4	5′AAGGAATACGCTTAAGCCCAAATGGCCTCAAATG3′
5	5′CGAGATCGGAATTCTAATACGACTCACTATAGGCCTGGACGAGAGGCGTG3′
6	5′CCAAATGGCCTCAATCGCCGCCCCTCGCCTCTTGCCGTGCGCGCTTCAGCACGACGAGTCCTGCGTCGATAAGGCGAATAGCGTATT3′
7	5′CGAGATCGCGGATCCTCTAGAAAGGGGACGGAAATATGG3′
8	5′CGAGATGCCGAATTCTAATACGACTCACTATAGGCTAGCCTGGACGAGAGGCGTG3′
9	5′GGCCTCAAATGTAATCGCCGCCCCTCGCCTCTTGCCGTGCGCGCTTCAGCAAGCCGAGTCCTCGCTCGATACATCTAAGGCG3′
10	5′CGAGATCGCGGATCCTCGAGTCTAGAAAGGGACGGAAATATGG3′
11	5′CGAGATGCCGAATTCTAATACGACTCACTATAGGCTAGCCTGGACGAGAGGCGTG3′
12	5′CATGGAATACGCTAGGACTTAGGAAGGAAAGGTTCCCAAACCAAGTTTCCCCGGAAAGGAACCCAAACCTTCCATATCCCAGCGTATTGCAGG3′
13	5′CGAGATCGCGGATCCTCGAGTCTAGAAAGGGACGGAAATATGG3′

*Eco*RI sites, and the *Hin*cII-*Bsi*YI fragment removed. Then, the *Mlu*I-*Eco*RI fragment of pUC-bcdIII was inserted back in a plasmid p875′ digested with *Mlu*I and *Eco*RI.

Plasmid Δ(IV+V)

The *Eco*RV-*Xmn*I fragment of p875′ was inserted in a pUC18 vector digested with *Hin*dIII and *Sma*I. This plasmid was digested with *Hin*dIII and the *Hin*fI-*Eco*RI fragment of *bcd* DNA was subcloned into it. The *Stu*I-*Sty*I fragment of this plasmid was then exchanged with the *Stu*I-*Sty*I fragment of the 875′ plasmid.

Plasmid ΔI series

The *Nla*IV-*Hin*dIII *bcd* fragment of the plasmid pDF 400, pDF495, pDF498 or pDF496 was subcloned into the *Stu*I-*Hin*dIII sites of the pUT7 vector, a pUC18 derivative containing a T7 RNA polymerase (kindly provided by A. Serganov) to create the RNAs ΔI wild-type, or mutants -(m,w), -(w,m), and -(m,m), respectively.

Plasmid III

The domain III fragment extends from position 231 to position 335, with a C to G 232 mutation designed to stabilized the stem of the helix. PCR amplification was performed using primers 3 (containing a T7 promotor) and 4 on plasmid 875. PCR products were purified on agarose gel.

Plasmid 875-HIV

A first PCR using primers 5 and 6 was used to introduce the HIV-1 DIS sequence within the *bcd* domain III at positions 251 and 304. This PCR generated a single-stranded product that was subsequently used in addition to primer 7 to generate a double-stranded DNA. This fragment was digested with *Eco*RI and *Bam*HI, and inserted in the vector pUC18 digested using the same restriction enzymes.

Plasmid 875-HIV′

The same strategy as above was used to substitute the *bcd* sequence between positions 257 and 298 by the HIV-1 DIS sequence, except that primers 8, 9 and 10 (instead of 5, 6 and 7) were used. Final PCR product was digested with *Nhe*I and *Xho*I.

Plasmid 875-L/R

The same strategy as above was used to substitute the *bcd* sequence between positions 232 and 332 by the tetraloop-receptor module sequence, using primers 11, 12 and 13. The final PCR product was digested with *Nhe*I and *Xho*I.

RNA synthesis and dimerization

Prior to transcription, every circular plasmid DNA was linearized using *Xba*I, except the plasmid ΔI series, which contained a *Hin*dIII restriction site. RNA III was directly transcribed with T7 RNA polymerase from the purified PCR product. *In vitro* transcription was conducted as described.[32] T7 RNA polymerase-His Tag was purified from the overproducing strain MC1061 transformed with pT7-911Q vectors, kindly supplied to us by T.E. Shrader, using a Ni + -NTA column. The RNA transcripts were purified using an FPLC system and a Bio-Sil TSK G2000 column in 200 mM sodium acetate (pH 5.8), 1% (v/v) methanol, 0.2 mM EDTA. Internally labeled RNAs were synthesized using [α-^{32}P]ATP (NEN) during transcription (37.5 μM [^{32}P]ATP; 50 μCi/μg of the DNA template).

In standard experiments, 0.6 μg of RNA dissolved in 16 μl of Milli-QS (Millipore) water was heated for three minutes at 85 °C and cooled slowly to 60 °C. After addition of the fivefold concentrated appropriate buffer, the samples were incubated for 30 minutes at 25 °C, then chilled on ice. Dimerization buffer (buffer D1) was: 50 mM sodium cacodylate (pH 7.5), 300 mM KCl, 5 mM $MgCl_2$. Monomer controls were obtained by replacing buffer D1 by buffer M1 (50 mM sodium cacodylate (pH 7.5), 40 mM KCl, 0.1 mM $MgCl_2$), The samples were analyzed by electrophoresis on 1% (w/v) agarose gel at room temperature. Electrophoresis buffer and gels contained 45 mM Tris borate (pH 8.3), 0.05 mM $MgCl_2$. The agarose gels were fixed for ten minutes in 10% (v/v) trichloroacetic acid and dried under vacuum.

K_d determination and derived procedures

The apparent dissociation constant (K_d) of the dimer was determined by mixing increasing concentration of unlabeled RNA (between 4.6 nM and 275 nM) with a negligible constant concentration of labeled RNA (<1 nM final). Dimerization was conducted under standard dimerization conditions (see above). Radioactivity was measured with a BAS 2000 BIO-Imager. The K_d was determined as described.[21] The fraction of dimer $f_D^{(w/w)}$ was defined as the weight-to-weight ratio of the dimer to the total RNA species.[21] All experiments were conducted at least three times. A difference of K_d was estimated to be significant when exceeding a factor of 2. Particular adaptations of the dimerization protocol (association and dissociation kinetic experiments) are described in Results.

Inhibition of RNA dimerization by oligonucleotides

The antisense oligonucleotide AS-LIIIb was complementary to nucleotides 270 to 283. The two sense RNAs were designed to mimic parts of domain III. The first one (S-LIIIb) mimics the apical loop IIIb (5′GCA UGC UCC ACU AAA GCC CGG GAA UAU GC3′) with a mutation (underlined) aimed to stabilize the stem. The second one (S-LIIIa) is a stem-loop closed by a GCAA tetraloop (underlined) containing the internal loop IIIa (5′GGA AUA CGC UAU UCG CCU CGC AAG AGG CCA UUU GGG CUU AAG CGU AUU CC3′). The correct folding of both sense RNAs was verified by enzymatic probing (data not shown). In a standard assay, ^{32}P-labeled RNA 875′ was allowed to dimerize at an RNA concentration of 215 nM. Increasing amounts of the unlabeled antisense oligonucleotides were added prior to the denaturation-renaturation step, or after the denaturation-renaturation step but before dimer formation, or after dimerization was completed for 30 minutes. When sense RNAs were used (LIIIb or S-LIIIa), target and sense RNAs were renatured separately, and added before or after the dimerization step. Dimerization of target RNA was followed as before.

Injection assays

In vitro synthesis of capped RNA was performed following instructions of Ambion using a cap analog (Amersham) in the presence of 2.5 mM Aminoallyl-UTP (Sigma) and 22.5 mM UTP. After phenol-extraction and precipitation, the fluorescent labeling of the RNA is performed by three hours of incubation at room temperature in 100 µl of 0.15 mM bicarbonate buffer (pH 9,0) in the presence of 5-l 5(6)Rox-SE (Molecular Probe). RNA was injected at a concentration of 1 µg/µl (in water) into less than one hour-old embryos[17] expressing either the Staufen-GFP fusion protein[24] or the tau-GFP fusion protein.[23] Confocal microscopy was performed on a Nikon Eclipse TE300 work station (Bio-Rad). Under standard conditions, observation was done for approximately 45 minutes after injection.

Acknowledgements

We acknowledge D. Ferrandon, P. Romby, R. Marquet and F. Brulé for fruitful discussions, and F. Winter for skilful technical assistance. C.W. is a recipient of Ministère de la Recherche et de la Technologie and of ''La Ligue contre le Cancer''. Some aspects of C.W's work were conducted with funding from a FEBS summer fellowship, and a Development Travelling fellowship.

References

1. Tomizawa, J. (1984). Control of ColE1 plasmid replication: the process of binding of RNA I and the primer transcript. *Cell,* **38**, 861-870.
2. Persson, C., Wagner, E. & Nordström, K. (1988). Control of replication of plasmid R1: kinetics of *in vitro* interaction between the antisense RNA, CopA, and its target, CopT. *EMBO J.* **7**, 3279-3288.
3. Siemering, K. R., Praszkier, J. & Pittard, A. J. (1994). Mechanism of binding of the antisense and target RNAs involved in the regulation of IncB plasmid replication. *J. Bacteriol.* **176**, 2677-2688.
4. Asano, K., Niimi, T., Yokoyama, S. & Mizobuchi, K. (1998). Structural basis for binding of the plasmid ColIb-P9 antisense Inc RNA to its target RNA with the 5′-rUUGGCG-3′ motif in the loop sequence. *J. Biol. Chem.* **273**, 11826-11838.
5. Asano, K. & Mizobuchi, K. (2000). Structural analysis of late intermediate complex formed between plasmid ColIb-P9 Inc RNA and its target RNA. How does a single antisense RNA repress translation of two genes at different rates? *J. Biol. Chem.* **275**, 1269-1274.
6. Isel, C., Westhof, E., Massire, C., Le Grice , S. F., Ehresmann, B., Ehresmann, C. & Marquet, R. (1999). Structural basis for the specificity of the initiation of HIV-1 reverse transcription. *EMBO J.* **18**, 1038-1048.
7. Berkhout, B. & van Wamel, J. L. B. (1996). Role of the DIS hairpin in replication of human immunodeficiency virus type 1. *J. Virol.* **70**, 6723-6732.
8. Clever, J., Wong, M. L. & Parslow, T. G. (1996). Requirement for kissing-loop-mediated dimerization of human immunodeficiency virus RNA. *J. Virol.* **70**, 5902-5908.
9. Haddrick, M., Lear, A. L., Cann, A. J. & Heaphy, S. (1996). Evidence that a kissing loop structure facilitates genomic RNA dimerisation in HIV-1. *J. Mol. Biol.* **259**, 58-68.
10. Paillart, J. C., Berthoux, L., Ottmann, M., Darlix, J. L., Marquet, R., Ehresmann, B. & Ehresmann, C. (1996). A dual role of the putative RNA dimerization initiation site of human immunodeficiency virus type 1 in genomic RNA packaging and proviral DNA synthesis. *J. Virol.* **70**, 8348-8354.
11. Zhang, F., Lemieux, S., Wu, X., St-Arnaud, D., McMurray, C. T., Major, F. & Anderson, D. (1998). Function of hexameric RNA in packaging of bacteriophage phi 29 DNA *in vitro*. *Mol. Cell,* **2**, 141-147.
12. Guo, P., Zhang, C., Chen, C., Garver, K. & Trottier, M. (1998). Inter-RNA interaction of phage phi29 pRNA to form a hexameric complex for viral DNA transportation. *Mol. Cell,* **2**, 149-155.
13. Chen, C., Sheng, S., Shao, Z. & Guo, P. (2000). A dimer as a building block in assembling RNA. A hexamer that gears bacterial virus phi29 DNA-translocating machinery. *J. Biol. Chem.* **275**, 17510-17516.
14. Ferrandon, D., Koch, I., Westhof, E. & Nusslein-Volhard, C. (1997). RNA-RNA interaction is required for the formation of specific *bicoid* mRNA 3′ UTR-STAUFEN ribonucleoprotein particles. *EMBO J.* **16**, 1751-1758.
15. St Johnston, D., Beuchle, D. & Nusslein-Volhard, C. (1991). Staufen, a gene required to localize maternal RNAs in the *Drosophila* egg. *Cell,* **66**, 51-63.
16. Micklem, D. R., Adams, J., Grunert, S. & St Johnston, D. (2000). Distinct roles of two conserved Staufen domains in *oskar* mRNA localization and translation. *EMBO J.* **19**, 1366-1377.
17. Ferrandon, D., Elphick, L., Nusslein-Volhard, C. & St Johnston, D. (1994). Staufen protein associates with the 3′UTR of *bicoid* mRNA to form particles that move in a microtubule-dependent manner. *Cell,* **79**, 1221-1232.
18. Macdonald, P. M. & Struhl, G. (1988). *Cis*-acting sequences responsible for anterior localization of *bicoid* mRNA in *Drosophila* embryos. *Nature,* **336**, 595-598.
19. MacDonald, P. M. (1990). *bicoid* mRNA localization signal: phylogenetic conservation of function and RNA secondary structure. *Development,* **110**, 161-171.
20. Seeger, M. A. & Kaufman, T. C. (1990). Molecular analysis of the *bicoid* gene from *Drosophila pseudoobscura*: identification of conserved domains within coding and noncoding regions of the *bicoid* mRNA. *EMBO J.* **9**, 2977-2987.
21. Paillart, J. C., Skripkin, E., Ehresmann, B., Ehresmann, C. & Marquet, R. (1996). A loop-loop ''kissing'' complex is the essential part of the dimer linkage of genomic HIV-1 RNA. *Proc. Natl Acad. Sci. USA,* **93**, 5572-5577.
22. Eguchi, Y. & Tomizawa, J. (1991). Complexes formed by complementary RNA stem-loops. Their formations, structures, and interactions with ColE1 Rom protein. *J. Mol. Biol.* **220**, 831-842.
23. Brand, A. (1995). GFP in *Drosophila*. *Trends Genet.* **11**, 324-325.
24. Micklem, D. R., Dasgupta, R., Elliott, H., Gergely, F., Davidson, C., Brand, A. *et al*. (1997). The *mago nashi* gene is required for the polarisation of the oocyte and the formation of perpendicular axes in *Drosophila*. *Curr. Biol.* **7**, 468-478.
25. Costa, M. & Michel, F. (1997). Rules for RNA recognition of GNRA tetraloops deduced by in vitro selection: comparison with *in vivo* evolution. *EMBO J.* **16**, 3289-3302.

26. Jaeger, L., Westhof, E. & Leontis, N. B. (2001). TectoRNA: modular assembly units for the construction of RNA nano- objects. *Nucl. Acids Res.* **29**, 455-463.
27. Jossinet, F., Paillart, J. C., Westhof, E., Hermann, T., Skripkin, E., Lodmell, J. S. *et al*. (1999). Dimerization of HIV-1 genomic RNA of subtypes A and B: RNA loop structure and magnesium binding. *RNA,* **5**, 1222-1234.
28. Mujeeb, A., Clever, J., Billeci, T., James, T. & Parslow, T. (1998). Structure of the dimer initiation complex of HIV-1 genomic RNA. *Nature Struct. Biol.* **5**, 432-436.
29. Dardel, F., Marquet, R., Ehresmann, C., Ehresmann, B. & Blanquet, S. (1998). Solution studies on the dimerization initiation site (DIS) of HIV-1 genomic RNA. *Nucl. Acids Res.* **15**, 3567-3571.
30. Paillart, J. C., Marquet, R., Skripkin, E., Ehresmann, B. & Ehresmann, C. (1994). Mutational analysis of the bipartite dimer linkage structure of human immunodeficiency virus type 1 genomic RNA. *J. Biol. Chem.* **269**, 27486-27493.
31. Skripkin, E., Paillart, J. C., Marquet, R., Ehresmann, B. & Ehresmann, C. (1994). Identification of the primary site of the human immunodeficiency virus type 1 RNA dimerization *in vitro*. *Proc. Natl Acad. Sci. USA,* **91**, 4945-4949.
32. Paillart, J. C., Westhof, E., Ehresmann, C., Ehresmann, B. & Marquet, R. (1997). Non-canonical interactions in a kissing loop complex: the dimerization initiation site of HIV-1 genomic RNA. *J. Mol. Biol.* **270**, 36-49.
33. Skripkin, E., Paillart, J. C., Marquet, R., Blumenfeld, M., Ehresmann, B. & Ehresmann, C. (1996). Mechanisms of inhibition of in vitro dimerization of HIV type I RNA by sense and antisense oligonucleotides. *J. Biol. Chem.* **271**, 28812-28817.
34. Lodmell, J. S., Ehresmann, C., Ehresmann, B. & Marquet, R. (2000). Convergence of natural and artificial evolution on an RNA loop-loop interaction: the HIV-1 dimerization initiation site. *RNA,* **6**, 1267-1276.
35. Laughrea, M. & Jetté, L. (1994). A 19-nucleotide sequence upstream of the 5′ major splice donor site is part of the dimerization domain of human immunodeficiency virus 1 genomic RNA. *Biochemistry,* **33**, 13464-13474.
36. Muriaux, D., Girard, P. M., Bonnet-Mathonière, B. & Paoletti, J. (1995). Dimerization of HIV-1lai RNA at low ionic strength. *J. Biol. Chem.* **270**, 8209-8216.
37. Muriaux, D., de Rocquigny, H., Roques, B.-P. & Paoletti, J. (1996). NCp7 activates HIV-1_{lai} RNA dimerization by converting a transient loop-loop complex into a stable dimer. *J. Biol. Chem.* **271**, 33686-33692.
38. Fu, W., Gorelick, R. J. & Rein, A. (1994). Characterization of human immunodeficiency virus type 1 dimeric RNA from wild-type and protease-defective virions. *J. Virol.* **68**, 5013-5018.
39. Kolb, F. A., Malmgren, C., Westhof, E., Ehresmann, C., Ehresmann, B., Wagner, E. G. & Romby, P. (2000). An unusual structure formed by antisense-target RNA binding involves an extended kissing complex with a four-way junction and a side-by-side helical alignment. *RNA,* **6**, 311-324.
40. Kolb, F. A., Engdahl, H. M., Slagter-Jager, J. G., Ehresmann, B., Ehresmann, C., Westhof, E. *et al*. (2000). Progression of a loop-loop complex to a four-way junction is crucial for the activity of a regulatory antisense RNA. *EMBO J.* **19**, 5905-5915.
41. Ramos, A., Grunert, S., Adams, J., Micklem, D. R., Proctor, M. R. & Freund, S. *et al*. (2000). RNA recognition by a Staufen double-stranded RNA-binding domain. *EMBO J.* **19**, 997-1009.
42. Temin, H. M. (1991). Sex and recombination in retroviruses. *Trends Genet.* **7**, 71-74.
43. Darlix, J. L., Lapadat-Tapolski, M., de Rocquigny, H. & Roques, B. P. (1995). First glimpses at structure-function relationships of the nucleocapsid protein of retroviruses. *J. Mol. Biol.* **254**, 523-537.
44. Gorelick, R. J., Nigida, S. M., Jr, Arthur, L. O., Henderson, L. E. & Rein, A. (1990). Roles of nucleocapsid cysteine arrays in retroviral assembly and replication: possible mechanisms in RNA encapsidation. In *Advances in Molecular Biology and Targeted Treatment of AIDS* (Kumar, A., ed.), pp. 257-272, Plenum Press, New York.
45. McBride, M. S. & Panganiban, A. T. (1996). The human immunodeficiency virus type 1 encapsidation site is a multipartite RNA element composed of functional hairpin structures. *J. Virol.* **70**, 2963-2973.
46. Guo, P. X., Bailey, S., Bodley, J. W. & Anderson, D. (1987). Characterization of the small RNA of the bacteriophage phi 29 DNA packaging machine. *Nucl. Acids Res.* **15**, 7081-7090.
47. Zhang, F. & Anderson, D. (1998). *In vitro* selection of bacteriophage phi29 prohead RNA aptamers for prohead binding. *J. Biol. Chem.* **273**, 2947-2953.
48. Bashirullah, A., Cooperstock, R. L. & Lipshitz, H. D. (1998). RNA localization in development. *Annu. Rev. Biochem.* **67**, 335-394.
49. Macdonald, P. M. & Kerr, K. (1997). Redundant RNA recognition events in *bicoid* mRNA localization. *RNA,* **3**, 1413-1420.
50. Maniatis, T., Fritsch, E. F. & Sambrook, J. (1982). *Molecular Cloning: A Laboratory Manual*, Cold Spring Harbor Laboratory Press, Cold Spring Harbor, NY.

Edited by J. Doudna

(Received 12 April 2001; received in revised form 27 August 2001; accepted 31 August 2001)